

## Electrochemical and spectroscopic studies on the interaction of europium-(9-acridine carboxylate)<sub>2</sub> complex with calf thymus DNA

Belal H. M. Hussein<sup>1,2,\*</sup>, Mostafa A Gouda<sup>1</sup>, and Abdullah I. El-Falouji<sup>3</sup>

<sup>1</sup> Chemistry Department, Faculty of Science & Art, Al Ula, Taibah University, Al Madinah Al Munawarh, KSA.

<sup>2</sup> Chemistry Department, Faculty of Science, Suez Canal University, Ismailia 41522, Egypt.

<sup>3</sup> Biotechnology Research Center, Suez Canal University, Ismailia 41522, Egypt.

\*E-mail: [belalhussein102@yahoo.com](mailto:belalhussein102@yahoo.com)

Received: 25 June 2017 / Accepted: 15 August 2017 / Published: 12 September 2017

---

A new europium-acridine-9-carboxylate (Eu(III)-(9-ACA)<sub>2</sub>(NO<sub>3</sub>)) was synthesized and characterized. The interaction of calf thymus DNA (ct-DNA) with Eu(III)-(9-ACA)<sub>2</sub>(NO<sub>3</sub>) has been investigated using UV-visible and fluorescence spectroscopic and electrochemical techniques including cyclic voltammetry and differential pulse voltammetry (DPV) on the GCE. UV-absorption spectroscopic techniques were employed to investigate the interaction between the Eu(III)-(9-ACA)<sub>2</sub>(NO<sub>3</sub>) and ct-DNA. Based on electrochemical and spectroscopic data, the mode of binding of Eu(III)-(9-ACA)<sub>2</sub>(NO<sub>3</sub>) to DNA through intercalation interaction was concluded. The stoichiometric coefficient (n) and apparent binding constant (β) were calculated to be 1.4 and 9.1 × 10<sup>4</sup> M<sup>-1</sup>, respectively. The antitumor activity of the complex against MDA-MB-231 (mammary cancer) and PC-3 (prostate carcinoma) cell lines was evaluated and the results showed promising activities.

---

**Keywords:** Europium-(9-acridine carboxylate)<sub>2</sub>; DNA interaction; voltammetry; Absorption and fluorescence spectra; Anti-tumor activities.

### 1. INTRODUCTION

Extensive efforts have been employed to kill the cancer cells with minimal side effects, because of cancer still causes to death and approximately more than half of cancer patients die from cancer diseases [1]. Therefore, the search for novel and selective anticancer drugs has attracted a great deal of interest in modern cancer research. The most important cell cycle target of many anticancer drugs is DNA binding with small molecule for the development of new anticancer drugs [2-5].

Rare earth complexes manifest antitumor activity. Moreover, recent different studies found that rare earth ions and their complexes strongly react with nucleic acids to inhibit the cancer cell divisions and act as chemical nucleases [6-7]. Therefore, tremendous interests have been drawn in recent years to study the anticancer activity of rare earth complexes [8-11].

Anticancer drugs interact with DNA via different binding modes such as intercalate, static, and grooves. A variety of techniques have been employed to investigate these binding modes. Among these techniques, the electrochemical investigations have been gained the most interest due to their selectivity, accuracy, a good evidence for the interaction mechanism and sharing similar principle of oxidation mechanism in the body and on the electrode [12]. Electrochemical approach can also be used for the quantification of these drugs [13-14].

Acridine derivatives are widely utilized as anticancer, antibacterial, antiprotozoal, and antimalarial drugs, [15-19]. Recently, 9-acridine derivatives strongly intercalated and had high binding affinities to nucleic acid [19-21]. These findings directly identify acridine derivatives as anticancer agents. The attempt to combine the 9-acridine moiety with lanthanide ions may be useful to possess high tumor cell growth inhibition activities.

In this work, the interaction of Eu(III)-(9-ACA)<sub>2</sub>(NO<sub>3</sub>), a potent anti-tumor drug, with double stranded calf thymus DNA (ds-DNA) was investigated by electrochemical methods included cyclic (CV) and differential pulse voltammetry (DPV) on a glassy carbon electrode (GCE). Absorption spectroscopy was carried to investigate the binding mechanism. The diffusion coefficients for oxidized species were calculated in the absence and presence of ds-DNA. Furthermore, the antitumor activities of the Eu(III)-complex against two cell lines were also examined and the results showed promising activities.

## 2. EXPERIMENTAL

### 2.1. Materials and Reagents

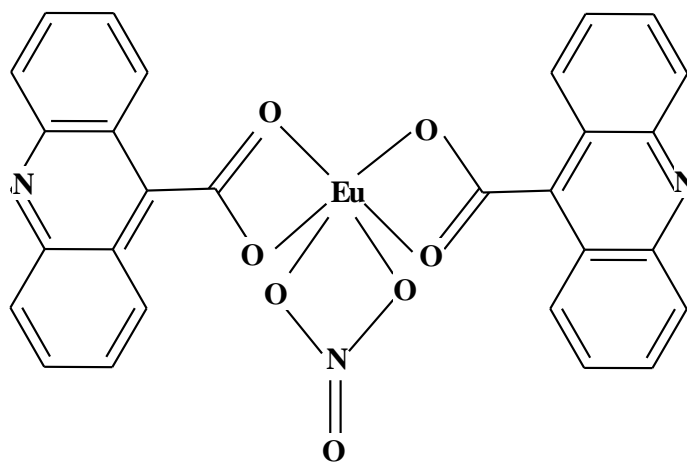


**Figure 1.** Suggested structure of the Eu(III) (9-ACA)<sub>2</sub>(NO<sub>3</sub>) complex

9-acridine carboxylic acid (9-ACA), Calf thymus deoxyribonucleic acid (ct-DNA), and Europium(III)nitrate ( $\text{Eu}(\text{NO}_3)_3 \cdot 6\text{H}_2\text{O}$ ) were purchased from Sigma.  $\text{Eu}(\text{III})(9\text{-ACA})_2(\text{NO}_3)$  complex was synthesized and characterized as reported in the literature [22, 23]. The structure of  $\text{Eu}(\text{III})(9\text{-ACA})_2(\text{NO}_3)$  complex (Fig. 1) was confirmed from analytical analysis, FTIR, and thermal analysis. All other reagents and solvents were analytical grade reagents. Double deionized water was used for all experiments. The stock solution of ct-DNA was prepared and stored in refrigerator at  $4^\circ\text{C}$  until used. The purity and concentration of DNA solution, expressed in M of nucleotide phosphate (NP), was determined by spectrophotometrical measurements [24, 25].

## 2.2. Apparatus

Voltammetry measurements were carried out using a 270 Electrochemistry System (EG&G, USA) in which a three-electrode system was used. A platinum wire was used as a counter electrode, a saturated calomel electrode (SCE) was used as a reference electrode and a glassy carbon electrode was used as a working electrode, electrode. Absorption, fluorescence and pH measurements were performed on a Perkin-Elmer lambda 20 UV-Vis spectrophotometer, Jasco-6300 spectrofluorometer, and (pH-220 L) pH-meter, respectively.

## 2.3. Antibacterial activity

In vitro antibacterial activities of Acridine-9-carboxylic acid and its  $\text{Eu}(\text{III})(9\text{-ACA})_2(\text{NO}_3)$  complex were investigated by using the Minimum inhibitory concentration (MIC) method [26,27] against *Pseudomonas aeruginosa* and *Staphylococcus aureus* as pathogenic strains.

## 2.4. Antitumor activity

The cytotoxicity activities of  $\text{Eu}(\text{III})(9\text{-ACA})_2(\text{NO}_3)$  complex and 9-ACA free ligand were screened in vitro against two human tumor cell lines including MDA-MB-231 (breast cancer) and PC-3 (prostate cancer) which were obtained from the National Cancer Institute (NCI, Cairo, Egypt). Tumor cells were cultured and cytotoxicity activities were evaluated by using MTT method assay as previously reported [28].

# 3. RESULTS AND DISCUSSION

## 3.1. Electrochemical behavior of $\text{Eu}(\text{III}) - (9\text{-ACA})_2(\text{NO}_3)$ complex

The electrochemical behavior of  $\text{Eu}(\text{III})(9\text{-ACA})_2(\text{NO}_3)$  binary system was investigated at the GCE using cyclic voltammetry technique, recorded in the 0.1 M acetate buffer solution (pH 4.8) at the scan rate of  $150 \text{ mVs}^{-1}$  within the electrode potential range of  $-0.30$  to  $-0.90 \text{ V}$  (Fig. 2). Under the

selected conditions, the cyclic voltammetry of Eu(III)-(9-ACA)<sub>2</sub>(NO<sub>3</sub>) in acetate buffer solution (pH= 5) exhibited only one cathodic current peak at potential of -775 mV, indicating that the reduction process of Eu(III)-(9-ACA)<sub>2</sub>(NO<sub>3</sub>) complex at GCE is an irreversible process. The cyclic voltammogram of the free ligand (9-acridine carboxylic acid) is conducted on the surface of glassy carbon electrode in the buffer solution (pH=5) at 25 °C. The free ligand doesn't exhibit reduction or oxidation peak within the studied potential range -0.30 to -0.90 V which corresponds to the electrochemical active range of Eu(III) metal ion under experimental condition.

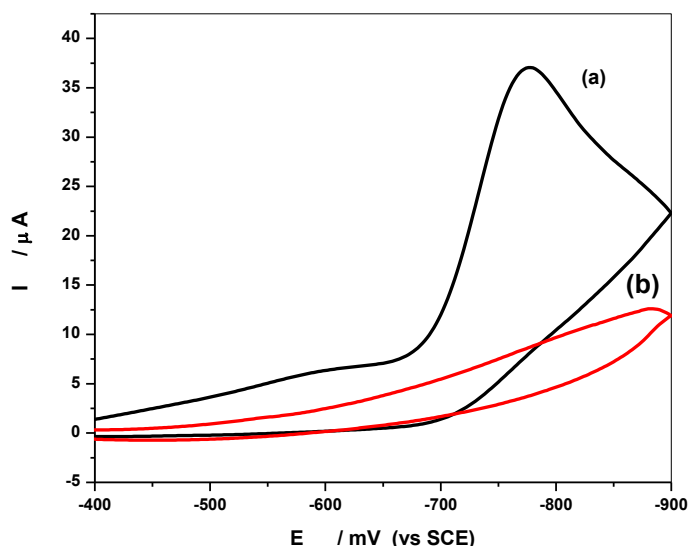


**Figure 2.** Cyclic voltammogram of Eu(III)(9-ACA)<sub>2</sub>(NO<sub>3</sub>) complex (a) and 9-ACA (b) in 0.1 M acetate buffer (pH 5) at 150 mVs<sup>-1</sup> scan rate.

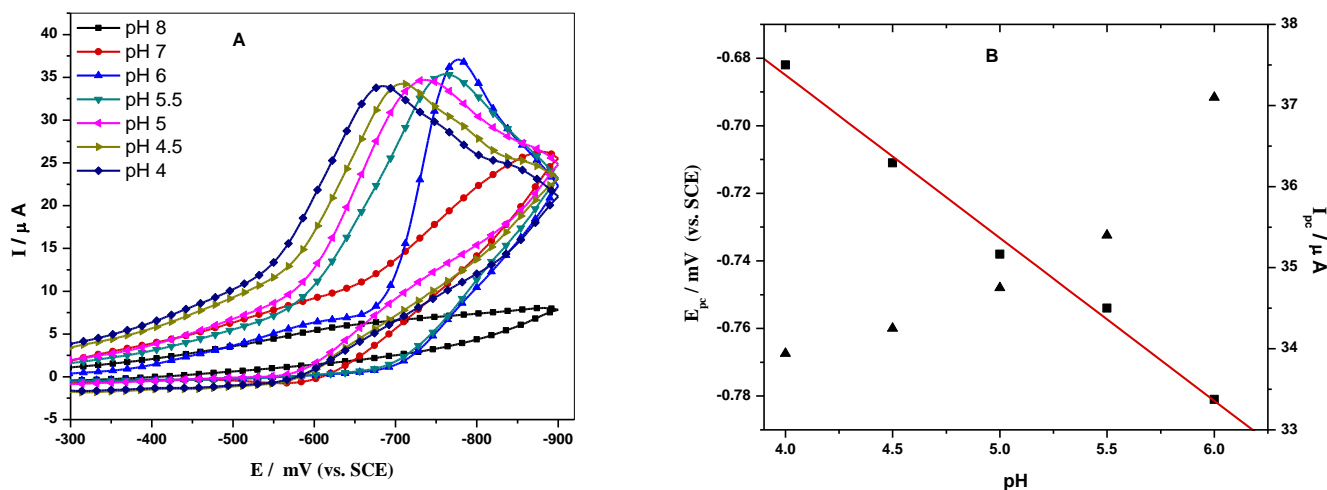


**Figure 3.** (A) Cyclic voltammogram of  $2.0 \times 10^{-5}$  M Eu(III) (9-ACA)<sub>2</sub>(NO<sub>3</sub>) complex in different pH values at 150 mVs<sup>-1</sup> scan rate. (B) Effect of pH values on the peak potential ( $E_{pc}$ ) and current ( $I_{pc}$ ) for the reduction of Eu(III) (9-ACA)<sub>2</sub>(NO<sub>3</sub>) complex at GCE in 0.1M acetate buffer.

The effect of pH values on the cathodic peak currents and potentials of Eu(III)-(9-ACA)<sub>2</sub>(NO<sub>3</sub>) at GCE was investigated as shown in Fig. 3. The results show that the cathodic peak potentials and currents are dependent on the pH values. The cathodic potential is shifted linearly to negative with increasing pH values up to pH =6. At pH more than 6, the currents started to decrease. Therefore, pH from 4 to 6 can be considered as the optimized pH for further electrochemical investigation of Eu(III)-(9-ACA)<sub>2</sub>(NO<sub>3</sub>) at GCE .

### 3.2. Electrochemical behavior of Eu(III)(9-ACA)<sub>2</sub>(NO<sub>3</sub>) with ds-DNA

The interaction between Eu(III)(9-ACA)<sub>2</sub>(NO<sub>3</sub>) complex and ct-DNA was investigated using CV and DP voltammetry techniques. The cyclic voltammogram representing the interaction of synthetic Eu(III)(9-ACA)<sub>2</sub>(NO<sub>3</sub>) complex with a series of ds-DNA concentrations in acetate buffer (pH 4.8) at 25 °C is depicted in Fig. 4. The electrochemical process of Eu(III)(9-ACA)<sub>2</sub>(NO<sub>3</sub>) complex with DNA at GCE is also irreversible. The reduction peak potential of Eu(III)(9-ACA)<sub>2</sub>(NO<sub>3</sub>) complex in the presence of ds-DNA shifts to more positive value from -775 mV to -746 mV which indicates the increase of DNA binding probability to Eu(III)(9-ACA)<sub>2</sub>(NO<sub>3</sub>) complex. Upon increasing the concentration of DNA to the complex, the cathodic peak current is decreased confirming the binding of the complex to DNA. Also, the decreasing of I<sub>pc</sub> can be attributed to the slow diffusion of the metal complexes bound to the slowly diffusing DNA. Thus, the binding of the Eu(III)(9-ACA)<sub>2</sub>(NO<sub>3</sub>) to nucleic acids may be related to the intercalation interaction with DNA as reported in the literatures [29-32].

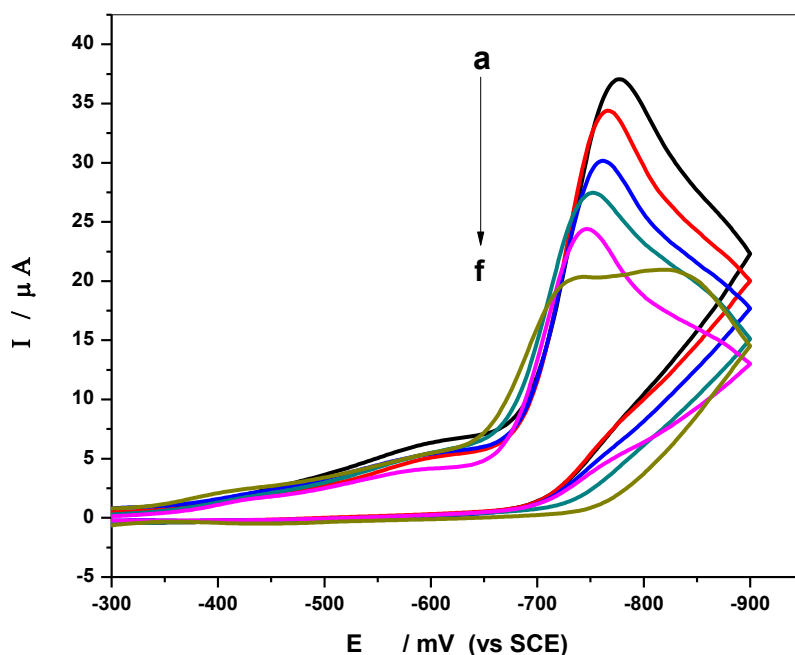


**Figure 4.** Cyclic voltammograms of  $2.0 \times 10^{-5}$  M Eu(III)(9-ACA)<sub>2</sub>(NO<sub>3</sub>) complex + ds-DNA in 0.1 M acetate buffer solution (pH 5) in the presence of (a) 0, (b) 1.5, (c) 3.0, (d) 4.4, e) 5.9, and (f)  $7.3 (\times 10^{-6})$  M ds-DNA. Scan rate:  $150 \text{ mVs}^{-1}$ .

Confirmation of the formation of DNA- Eu(III)(9-ACA)<sub>2</sub>(NO<sub>3</sub>) complex in solution has been investigated using DPV on a GCE. As the sensitivity of DPV was better than that of CV. DPV curves of Eu(III)(9-ACA)<sub>2</sub>(NO<sub>3</sub>) complex in the absence and presence of DNA are shown in Fig. 5. The peak current of Eu(III)(9-ACA)<sub>2</sub>(NO<sub>3</sub>) complex appears at the potential of -0.623 V. The peak potential (E<sub>p</sub>) shifted positively (E<sub>p</sub> = -0.600 V) and the peak current is decreased with the addition of ds-DNA. This finding strongly supports the interaction between ds-DNA and Eu(III)(9-ACA)<sub>2</sub>(NO<sub>3</sub>) and suggested that a new complex was formed between Eu(III)(9-ACA)<sub>2</sub>(NO<sub>3</sub>) and DNA [29,32-34].

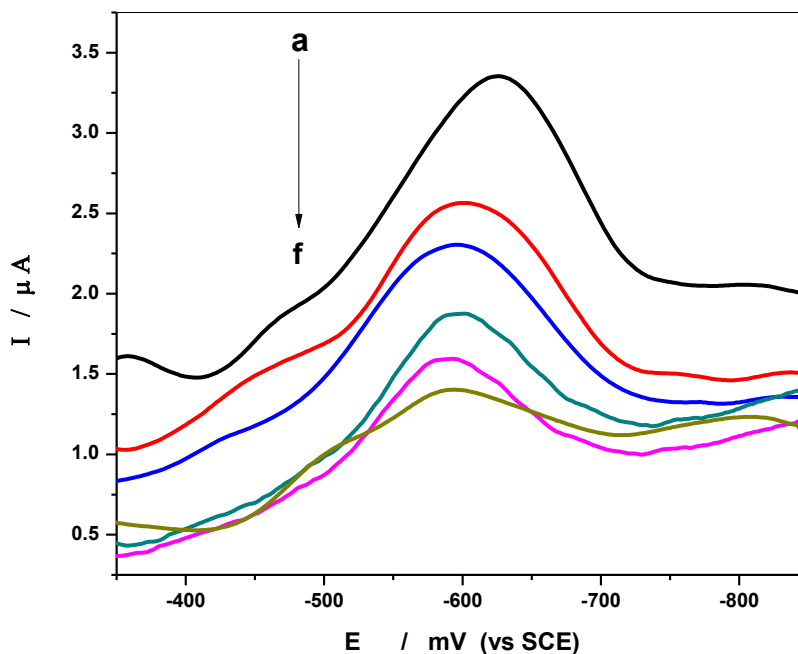
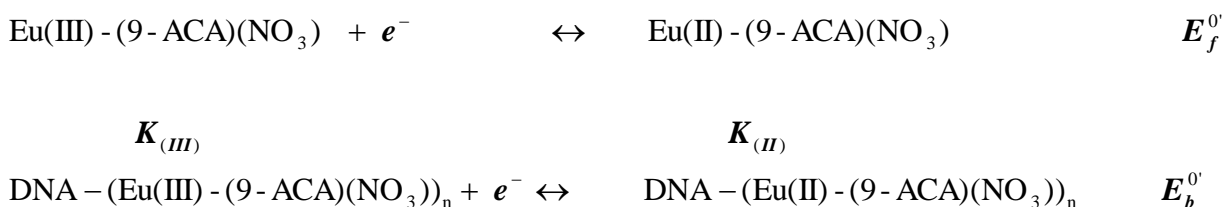


**Figure 5.** Differential pulse voltammetry of Eu(III) (9-ACA)<sub>2</sub>(NO<sub>3</sub>) complex in the absence (a) and presence of ds-DNA in 0.1M acetate buffer at pH 5.

The electrochemical processes of Eu(III)(9-ACA)<sub>2</sub>(NO<sub>3</sub>) complex and DNA can be represented by a square Scheme according to the literature [35, 36] as shown bellow



The change in potential is related to binding constant and can be used to determine the equilibrium constants for the interaction of Eu(II) complex to ct-DNA as follows [35, 36]:

$$E_b^{0'} - E_f^{0'} = RT / nF \ln(K_{II} / K_{III}) \tag{1}$$

where  $E_b^{0'}$  and  $E_f^{0'}$  are formal potentials of the Eu(III)/Eu(II)-complex in the bound and free form, respectively. The ratio of the binding constants ( $K_{II}/K_{III}$ ) of Eu(III)/Eu(II) complexes for DNA binding is found to be less than unity (for limiting shift of -23 mV,  $K_{II}/K_{III}$  is  $1.3 \times 10^{-4}$ ), indicating that binding of Eu(II)-complex (reduced form) to DNA is small compared to that of Eu(III)-complex (oxidized form).

3.3. Determination of the binding constant and stoichiometric coefficient between Eu(III) (9-ACA)<sub>2</sub>(NO<sub>3</sub>) and ds-DNA

Assuming that Eu(III)(9-ACA)<sub>2</sub>(NO<sub>3</sub>) complex reacts with ct-DNA producing only a single complex of DNA-(Eu(III)(9-ACA)<sub>2</sub>(NO<sub>3</sub>))<sub>n</sub> [37, 38], a reaction equation is as follows:



The apparent binding constant,  $\beta$ , is given by

$$\beta^n = \frac{[\text{DNA} - (\text{Eu(III) - complex})n]}{[\text{Eu(III) - complex}]^n [\text{DNA}]} \tag{3}$$

where [Eu(III)-complex] and [DNA] are the free concentration of Eu(III)(9-ACA)<sub>2</sub>(NO<sub>3</sub>) and ct-DNA at equilibrium, respectively. [DNA-(Eu(III)-complex)n] and n are the concentration of the formed complex and the stoichiometric coefficient, respectively. The fraction of DNA bound in the complex is given by

$$f = \frac{[\text{DNA} - (\text{Eu(III) - complex})n]}{[\text{DNA} - (\text{Eu(III) - complex})n]_{\text{max}}} = \frac{[\text{DNA} - (\text{Eu(III) - complex})n]}{[\text{DNA}]_0} \tag{4}$$

where [DNA]<sub>0</sub> is the total concentration of ct-DNA and [DNA-(Eu(III)-complex)n]<sub>max</sub> is the maximum concentration of DNA-(Eu(III)-complex)n. The total concentration of the ct-DNA is

$$[\text{DNA}]_0 = [\text{DNA}] + [\text{DNA} - (\text{Eu(III) - complex})n] \tag{5}$$

Insertion of Eqs 4 and 5 into Eq.3 leads to

$$\begin{aligned} \beta^n &= \frac{1}{[\text{Eu(III) - complex}]^n} \cdot \frac{[\text{DNA} - (\text{Eu(III) - complex})n]}{([\text{DNA}]_0 - [\text{DNA} - (\text{Eu(III) - complex})n])} \\ \beta^n [\text{Eu(III) - complex}]^n &= \frac{[\text{DNA} - (\text{Eu(III) - complex})n]}{([\text{DNA}]_0 - [\text{Eu(III) - complex})n])} \\ &= \frac{[\text{DNA} - (\text{Eu(III) - complex})n]/[\text{DNA}]_0}{([\text{DNA}]_0 - [\text{DNA} - (\text{Eu(III) - complex})n])/[\text{DNA}]_0} = \frac{f}{1 - f} \end{aligned} \tag{6}$$

Then, the following logarithmic equation can be deduced from the above equation:

$$\log\left(\frac{f}{1-f}\right) = n \log(\beta / M^{-1}) + n \log([\text{Eu(III) - complex}]^n / M) \tag{7}$$

It is assumed that the changes in the current is due to the presence a concentration of DNA over different concentrations of the Eu(III)(9-ACA)<sub>2</sub>(NO<sub>3</sub>) complex. Thus, the decreasing value of the peak current is proportional to the concentration of DNA-(Eu(III)(9-ACA)<sub>2</sub>(NO<sub>3</sub>))<sub>n</sub> complex:

$$\Delta I = k [\text{DNA} - (\text{Eu(III) - complex})n] \tag{8}$$

$\Delta I (= I^0 - I)$  is the change in cathodic peak current of Eu(III)(9-ACA)<sub>2</sub>(NO<sub>3</sub>) upon each addition of ct-DNA.  $I^0$  and  $I$  are cathodic peak current of Eu(III)(9-ACA)<sub>2</sub>(NO<sub>3</sub>) in the absence and presence of ct-NA, respectively.  $\Delta I_{\text{max}}$  is the same parameter when the compound is totally bound to ct-DNA.

$$\Delta I_{\text{max}} = k [\text{DNA}]_o \tag{9}$$

Therefore,  $(\Delta I / \Delta I_{\text{max}})$  denotes the fraction of Eu(III)(9-ACA)<sub>2</sub>(NO<sub>3</sub>) bound to DNA.

$$f = \Delta I / \Delta I_{\text{max}} \tag{10}$$

Insertion of Eq. (10) into Eq. (7), the following equation can be yielded:

$$\log\frac{\Delta I}{(\Delta I_{\text{max}} - \Delta I)} = n \log(\beta / M^{-1}) + n \log([\text{Eu(III) - complex}] / M) \tag{11}$$

The Eqs 8 and 9 are deduced to Eq. 3 and then, the following equation can be deduced:

$$\beta^n = \frac{\Delta I}{(\Delta I_{\text{max}} - \Delta I) [\text{Eu(III) - complex}]^n} \tag{12}$$

$$\frac{(\Delta I_{\text{max}} - \Delta I)}{\Delta I} = \frac{1}{\beta^n [\text{Eu(III) - complex}]^n} \tag{13}$$

$$\frac{\Delta I_{\text{max}}}{\Delta I} - 1 = \frac{1}{\beta^n [\text{Eu(III) - complex}]^n} \tag{14}$$

$$\frac{1}{(\Delta I)} = \frac{1}{(\Delta I_{\text{max}})} + \frac{1}{(\Delta I_{\text{max}})(\beta)^n ([\text{Eu(III) - complex}])^n} \tag{15}$$

The equations 11 and 15 can be applied to evaluate the binding constant and molar ratio [30, 39-44]. The voltammetric titration was employed to determine the binding constant (K) and stoichiometric coefficient (n). According to Eq. 11, the relationship curve of  $\log (\Delta I / (\Delta I_{\text{max}} - \Delta I))$  and

$\log [\text{Eu(III)-complex} / \text{M}]$  should be a straight line with the suitable  $n$ , if there is only one complex formed. Fig. 6 depicts a plot of  $\log (\Delta I / (\Delta I_{\text{max}} - \Delta I))$  as a function of  $\log [\text{Eu(III)-complex} / \text{M}]$  for DNA-Eu(III) (9-ACA)(NO<sub>3</sub>) system. From the intercept and slope values the binding constant at room temperature was determined to be  $9.1 \times 10^4 \pm 300 \text{ M}^{-1}$  in 0.1M acetate buffer with 1.4 stoichiometric coefficient. This value is in accordance with the previous study for the intercalation and groove binding of small molecule into the DNA molecules [23,34,45,46].

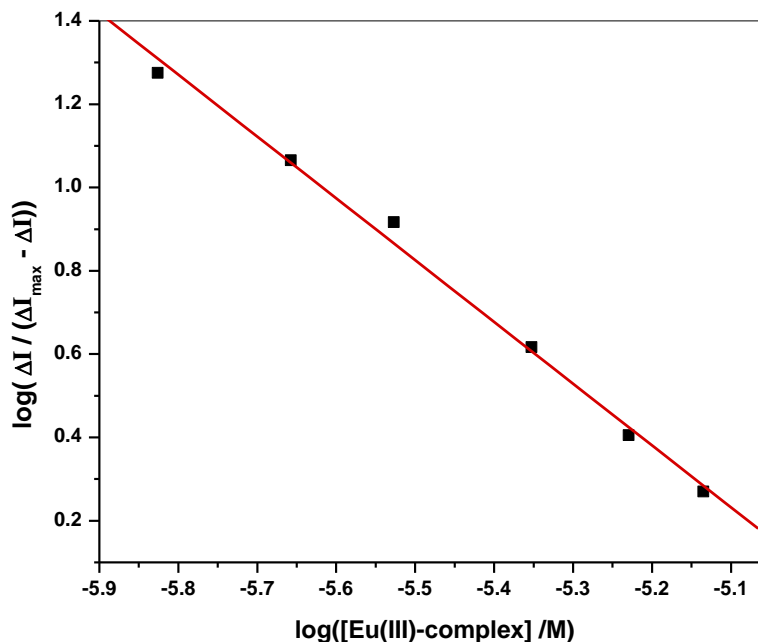


**Figure 6.** Dependence of  $\log (\Delta I / (\Delta I_{\text{max}} - \Delta I))$  on  $\log [\text{Eu(III)-complex} / \text{M}]$

### 3.4. Effect of scan rates

The effects of scan rate ( $\nu$ ) on the reduction peak currents and reduction peak potentials were investigated to assess the interaction of  $\text{Eu(III)(9-ACA)}_2(\text{NO}_3)$  with ct-DNA. The diffusion coefficients for oxidized and reduced species and can be calculated from the following equation [47]

$$I = 0.4463 \left( \frac{F^3}{RT} \right)^{1/2} n^{3/2} A_0 D^{1/2} C_0 \nu^{1/2} \tag{16}$$

where,  $I / \text{A}, n, A_0 / \text{cm}^2, D / \text{cm}^2 \text{ s}^{-1}, C_0 / \text{mole cm}^{-3}$ , and  $\nu / \text{Vs}^{-1}$  refer to the peak current, number of electrons involved in the reduction, area of the electrode, diffusion coefficient, concentration of electroactive species, and scan rate, respectively. One can get the value of  $0.4463(F^3/RT)^{1/2}$  as  $2.69 \times 10^5 \text{ A s (molV}^{1/2})^{-1}$ . Cyclic voltammograms of  $\text{Eu(III)(9-ACA)}_2(\text{NO}_3)$  complex in acetate buffer in the absence and presence of DNA have been recorded at different scan rates. The dependence of the cathodic peak potential on the square root of scan rate ( $\nu / \text{Vs}^{-1})^{1/2}$  is depicted in Fig.7A. The relationship between the reduction peak current and the square root of the scan

rate is linear, following equations below:  $I_{pc} = -4.32\mu A + \{102 [v/(V/s)]^{1/2}\}\mu A$  for  $\text{Eu(III)(9-ACA)}_2(\text{NO}_3)$  complex and  $I_{pc} = -3.07\mu A + \{88.9 [v/(V/s)]^{1/2}\}\mu A$  for DNA- $\text{Eu(III)(9-ACA)}_2(\text{NO}_3)$  system, suggesting that the redox processes of both free and bound  $\text{Eu(III)(9-ACA)}_2(\text{NO}_3)$  are under diffusion control. From the slope of the relationship between the current and the square root of the scan rate, the diffusion coefficient can be determined. This procedure gives diffusion coefficients of  $1.5 \times 10^{-9}$  and  $1.1 \times 10^{-9} \text{ cm}^2\text{s}^{-1}$  for the oxidized form of free and bound  $\text{Eu(III)(9-ACA)}_2(\text{NO}_3)$ , respectively. This indicates that the redox processes of both free and bound  $\text{Eu(III)(9-ACA)}_2(\text{NO}_3)$  are under diffusion control. The slope of the plot is lower in the presence of DNA, indicated lowering the diffusion coefficient of the DNA- $\text{Eu(III)(9-ACA)}_2(\text{NO}_3)$  complex in the bulk of the solution. The relationship of the peak potentials with scan rate was further constructed (Fig.7B), which obeys the following equations:  $E_{pc} = -0.843\text{V} - (0.046 \ln(v/V\text{s}^{-1})) \text{V}$  and  $E_{pc} = -0.850\text{V} - (0.042 \ln(v/V\text{s}^{-1}))\text{V}$  for  $\text{Eu(III)(9-ACA)}_2(\text{NO}_3)$  and DNA- $\text{Eu(III)(9-ACA)}_2(\text{NO}_3)$  system, respectively.

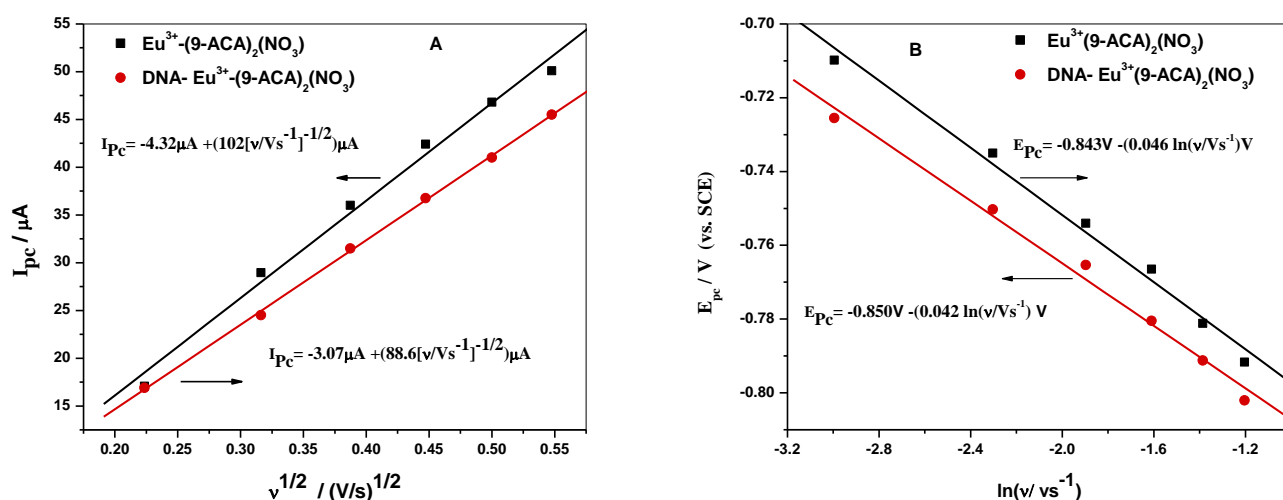


**Figure 7.** (A) Dependence of cathodic peak current ( $I_{pc}/\mu\text{A}$ ) on the square root of scan rate ( $(v/V\text{s}^{-1})^{1/2}$ ). (B) Correlation between cathodic peak potential ( $E_{pc}/\text{V}$ ) and  $\ln(v/V\text{s}^{-1})$  for  $\text{Eu(III)(9-ACA)}_2(\text{NO}_3)$  complex and DNA- $\text{Eu(III)(9-ACA)}_2(\text{NO}_3)$  complex in 0.1 M acetate buffer at 25.0 °C.

### 3.5. UV-vis absorption spectra

The metal complexes can interact with nucleic acids through intercalative, groove or electrostatic binding. The red shift and hypochromic effect were observed in the absorption spectra of the small molecules when the small molecule was intercalated into the space between two DNA base pairs, [48,49]. The absorption spectra of the interaction of  $\text{Eu(III)(9-ACA)}_2(\text{NO}_3)$  complex with ct-DNA are given in Fig. 8A. The absorption spectrum of  $\text{Eu(III)(9-ACA)}_2(\text{NO}_3)$  complex has an absorption peak at about 361 nm which is assigned to  $\pi-\pi^*$  transition. On addition of ct-DNA, the absorption spectrum of  $\text{Eu(III)-complex}$  demonstrated clear hypochromicity at the maximum absorbance with somewhat red shift from 361 to 365 nm. This finding suggested the formation of some

type of binding probably intercalation binding mode [50, 51]. Absorption titration measurements can be employed to determine the binding constant between Eu(III) (9-ACA)<sub>2</sub>(NO<sub>3</sub>)<sub>2</sub> complex and ct-DNA applying the following relationship [23]

$$\frac{1}{\Delta A} = \frac{1}{[\text{Eu(III) - complex}]_0} \left( \frac{1}{\Delta \epsilon} + \frac{1}{\Delta \epsilon K [\text{DNA}]_0} \right) \quad (17)$$

where  $\Delta \epsilon$  the difference between the molar absorption coefficients of Eu-complex and Eu-complex-DNA.  $\Delta A$  is the difference between the absorbance of Eu-complex in the presence and in the absence of DNA.  $[\text{Eu-complex}]_0$  and  $[\text{DNA}]_0$  are the initial concentration of Eu-complex and DNA, respectively. The plot of  $1/\Delta A$  versus  $1/[\text{DNA}]_0$  was linear (Fig. 8B). The binding constant was found to be  $6.7 \times 10^4 \text{ M}^{-1}$ . This value is comparable to that obtained from the voltammetric titration.

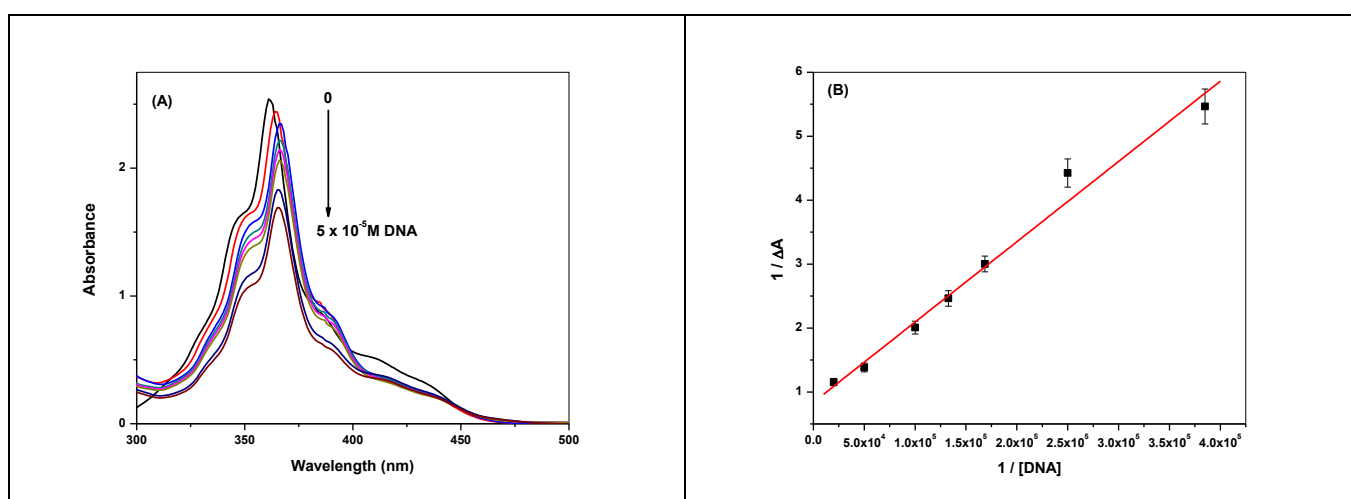


**Figure 8.** (A) Absorption spectra of Eu(III) (9-ACA)<sub>2</sub>(NO<sub>3</sub>)<sub>2</sub> complex in the absence and presence of ds-DNA in 0.1M acetate buffer at pH 5. (B) Double reciprocal plot (Benesi-Hildebrand plot)

### 3.7. Fluorescence spectra

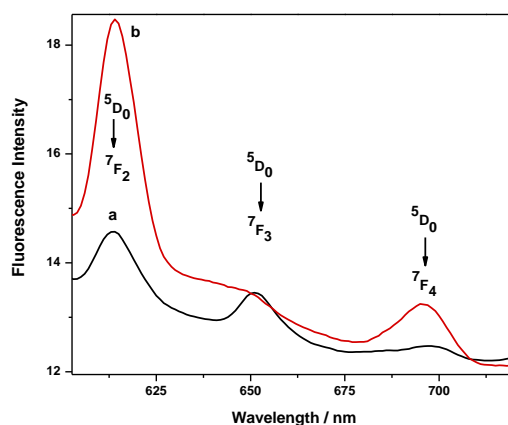


**Figure 9.** Fluorescence spectra of Eu(III) (9-ACA)<sub>2</sub>(NO<sub>3</sub>)<sub>2</sub> complex in the absence (a) and presence (b) of ds-DNA in 0.1M acetate buffer at pH 5. Excitation wavelength was 290 nm.

The fluorescence measurements for the interaction of  $\text{Eu(III)(9-ACA)}_2(\text{NO}_3)$  with DNA in 0.1M acetate buffer (pH=5) was monitored as described in Fig.9. Fluorescence spectrum of  $\text{Eu(III)(9-ACA)}_2(\text{NO}_3)$  complex exhibits the characteristic emission bands for  $\text{Eu}^{3+}$  ions [50] at 615 nm ( ${}^5\text{D}_0 \rightarrow {}^7\text{F}_2$ ) which is obviously higher than the other emission bands at 645 nm ( ${}^5\text{D}_0 \rightarrow {}^7\text{F}_3$ ), and 690 nm ( ${}^5\text{D}_0 \rightarrow {}^7\text{F}_4$ ). Addition of DNA to  $\text{Eu(III)}$ -complex leads to increase the emission bands of  $\text{Eu(III)}$  in the complex through the energy transfer. The fluorescence enhancement provided a strong interaction between  $\text{Eu(III)(9-ACA)}_2(\text{NO}_3)$  and DNA through intercalation binding mode [23,52].

### 3.8. Effect of $\text{Eu(III)}$ -complex on the microorganism

In the light of interesting antimicrobial activities of the coordination complex, the ligand and its corresponding  $\text{Eu(III)}$ -complex were evaluated their antibacterial activity against *Pseudomonas aeruginosa* and *Staphylococcus aureus* by MIC assay. In case of *Pseudomonas aeruginosa*, the complex (MIC =1600  $\mu\text{M}$ ) is more potent than the ligand (MIC=2100  $\mu\text{M}$ ). For *Staphylococcus aureus*, the complex (MIC = 2000 $\mu\text{M}$ ) is more potent active than ligand (MIC=2300  $\mu\text{M}$ ). The antimicrobial activity of the  $\text{Eu(III)(9-ACA)}_2(\text{NO}_3)$  complex against the *Pseudomonas aeruginosa* and *Staphylococcus aureus* is much higher than ligand only (Acridine-9-carboxylic acid).The antibacterial mechanism was hypothesized that the  $\text{Eu(III)(9-ACA)}_2(\text{NO}_3)$  complex has an effect on cell.

### 3.9. Antitumor activity

The antiproliferative of the ligand 9-ACA and  $\text{Eu(III)(9-ACA)}_2(\text{NO}_3)$  complex activities against MDA-MB-231 (mammary cancer) and PC-3 (human prostate carcinoma cell line) cancer cell lines were evaluated by the standard MTT assay with carboplatin as the positive control. The calculated  $\text{IC}_{50}$  values are listed in Table 1.  $\text{Eu(III)(9-ACA)}_2(\text{NO}_3)$  complex displayed a higher cytotoxic activity than the parent ligand.

**Table 1.** In vitro anticancer screening of the synthesized  $\text{Eu(III)(9-ACA)}_2(\text{NO}_3)$  complex and 9-ACA against MDA-MB-231 (mammary cancer) and PC-3 (human prostate carcinoma ) cell line.

Compound	MDA-MB-231 $\text{IC}_{50}$ $\mu\text{M}$	PC-3 $\text{IC}_{50}$ $\mu\text{M}$
9-Acridine carboxylic acid	$29.62 \pm 0.3 \mu\text{M}$	$40.7 \pm 0.2 \mu\text{M}$
$\text{Eu(III)(9-ACA)}_2(\text{NO}_3)$	$21.29 \pm 0.28 \mu\text{M}$	$26.0 \pm 0.88 \mu\text{M}$
Carboplatin	$14 \pm 0.28 \mu\text{M}$	$19 \pm 0.88 \mu\text{M}$

## 4. CONCLUSION

In this work, the reduction peak potential of the  $\text{Eu(III)(9-ACA)}_2(\text{NO}_3)$  complex is influenced by the pH values. DNA binding with  $\text{Eu(III)(9-ACA)}_2(\text{NO}_3)$  complex was demonstrated by

electrochemical, fluorescence, and absorption techniques. The results obtained indicate that there is a strong interaction between  $\text{Eu(III)(9-ACA)}_2(\text{NO}_3)$  complex and ct-DNA. The binding of  $\text{Eu(III)}$ -complex to ct-DNA is related to the intercalation interaction with DNA backbone. The DNA- $\text{Eu(III)(9-ACA)}_2(\text{NO}_3)$  complex interaction has an effect on the cell division of bacteria and tumor cells. This interaction can inhibit the replication process and prevent tumor and bacteria cells from dividing and producing more cells thence induce the programmed cell death (apoptosis) of tumor cell. This result suggests that a further clinical application of this synthetic compound have a strong potential as anti-tumor compounds.

#### ACKNOWLEDGMENTS

The authors thank the Deanship of Scientific Research at Taibah University in Saudi Arabia for funding this research, Grant Number 4590/1434.

#### References

1. A. Jemal, R. Siegel, E. M. Ward, M. J. Thun, *Am. Cancer Soc.*, 1 (2007), 1.
2. M.M. Ghoraba, F.A. Ragabb, H.I. Heibac, R.M. El-Hazekc, *Eur. J. Med. Chem.* 46 (2011) 5120.
3. D.M. Reddy, N. A. Qazi, S.D. Sawant, A.H. Bandey, J. Srinivas, M. Shankar, S.K. Singh, M. Verma, G. Chashoo, A. Saxena, D. Mondhe, A.K. Saxena, V.K. Sethi, S.C. Taneja, G.N. Qazi, H.M.S. Kumar, *Eur. J. Med. Chem.*, 46 (2011) 3210.
4. P. Krishnamoorthy, P. Sathyadevi, A.H. Cowley, R.R. Butorac, N. Dharmaraj, *Eur. J. Med. Chem.*, 46 (2011) 3376.
5. S. David, E. Meggers, *Curr. Opin. Chem. Biol.*, 12 (2008) 197.
6. X.Q. He, Q.Y. Lin, R.D. Hu, X.H. Lu, *Spectrochim. Acta A*, 68 (2007) 184.
7. J. Torres, M. Brusoni, F. Peluffo, C. Kremer, S. Dominguez, A. Mederos, E. Kremer, *Inorg. Chim. Acta*, 358 (2005) 3320.
8. I. Kostova, T. Stefanova, *J. Trace Elements, Med. Biol.*, 24 (2010) 7.
9. G.H. Zhao, F.H. Li, H. Lin, H.K. Lina, *J. Bioorg. Med. Chem.*, 15 (2007) 533.
10. Z.M. Wang, H.K. Lin, S.R. Zhu, T.F. Liu, Z.F. Zhou, R.T. Chen, *Anticancer Drug Des.*, 15 (2000) 405.
11. B. H. M. Hussein, H. A. Azab, M. F. El-Azab, A. I. El-Falouji, *Eur. J. Med. Chem.*, 51(2012) 99.
12. S. Rauf, J.J. Gooding, K. Akhtar, M.A. Ghauri, M. Rahman, M.A. Anwar, A.M.Khalid, *J. Pharma. Biomed. Anal.*, 37 92005) 205.
13. R. Sandulescu, I. Marianb, S. Mirel, R. Opreana, L. Roman, *J. Pharma. Biomed. Anal.*, 18 (1998)75.
14. L. Wang, L. Lin, B. Ye, *J. Pharma. Biomed. Anal.*, 42 (2006) 625.
15. M. Wu, W. Wu, X. Gao, X. Lin, Z. Xie, *Talanta*, 75 (2008) 995.
16. R. Liu, J. Yang, C. Sun, L. Li, X. Wu, Z. Li, C. Qi, *Chem. Phys. Lett.*, 376 (2003)108.
17. S.P. Liu, S. Chen, Z.F. Liu, X.L. Hu, T.S. Li, *Chim. Acta*, 535 (2005) 169.
18. M. Wang, J. Yang, X. Wu, F. Huang, *Anal. Chim. Acta*, 422 (2000)151.
19. G.J. Atwell, B.F. Cain, B.C. Baguley, G.J. Finlay, W.A. Denny, *J. Med. Chem.*, 27 (1984)1481.
20. D. Sabolova, M. Kozurkova, P. Kristian, I. Danihel, D. Podhradsky, J. Imrich, *Int. J. Biol. Macromol.*, 38 (2006) 94.
21. Y.Z. Quan, Z. Yun-You, N. Li, *J. Appl. Chem.*, 22 ( 2005) 1258.

22. H. A. Azab, B. H.M. Hussein, M. F. El-Azab, M. Gomaa, A. I. El-Falouji *Bioorganic & Medicinal Chemistry* 1, (2013) 223
23. H. A. Azab , B. H. M. Hussein , A. I. El-Falouji, *J. Fluorescence*, 22 (2012) 639
24. H. S. Wang, H.X. Ju, H.Y. Chen, *Electroanalysis* 131 (2001) 105.
25. J. Marmur, R. Rownd, C.L. Schildkraut, in *Progress in Nucleic Acid Research*, Vol. 1 (Eds: J.N. Davidson, W.E. Cohn), Academic Press, New York, 1963, p. 232.
26. R.N. Jones, A.L. Barry, T.L. Gaven, J.A. Washington, E.H. Lennette, A. Balows, W.J. Shadomy, *Manual of Clinical Microbiology*, 4th ed.; American Society for Microbiology: Washington, DC, 1984.
27. J.M. Andrews, *J. Antimicrob. Chemoth.*, 48 (2001) 5.
28. E. Tselepi-Kalouli, N. Katsaros, *J. Inorg. Biochem.*, 37(1989) 271.
29. C. W. Yaw, W. T. Tan, W. S. Tan, C. H. Ng, W. B. Yap, N. H. Rahman, M. Zidan, *Int. J. Electrochem. Sci.*,7(2012) 4692
30. M.T. Carter, M. Roderiguez, A.J. Bard, *J. Am. Chem. Soc.*, 111 (1989) 8901.
31. K. Zhang and W. Liu, *Int. J. Electrochem. Sci.*, 6 (2011) 4006.
32. N. Li, Y. Ma, C. Yang, L.P. Guo, X.R. Yang, *Biophys. Chem.*, 116 (2005) 199.
33. L.Sun, X. Wang, N. Zou, H. Li, and Z. Yu, *Int. J. Electrochem. Sci.*, 10 (2015) 7349.
34. Q. Wang, X. Wang, Z. Yu, X. Yuan, and K. Jiao *Int. J. Electrochem. Sci.*, 11(2011) 5470.
35. X. Lu, K. Zhu, M. Zhang, H. Liu, J.Kang, *J. Biochem. Biophys. Methods*, 52 (2002) 189.
36. J. Kang, L. Zhuo, X. Lu, H. Liu, M. Zhang, H. Wu, *J. Inorg. Biochem.*, 98, (2004) 79.
37. F. Wang, Y. Xu, J. Zhao, S. Hu, *Bioelectrochemistry* 71 (2006) 50.
38. H. Heli, S.Z. Bathaie, M.F. Mousavi, *Electrochem. Commun.*, 6 (2004) 1114.
39. Y.Q. Li, Y.J. Guoa, X.F. Li, J. H. Pan, *Talanta*, 71 (2007) 123.
40. X. Tian, Y. Song, H. Dong, B. Ye, *Bioelectrochemistry* 73 (2008) 18.
41. S. Niu, M. Wu, S. Bi, S. Zhang, *Bioelectrochemistry*, 73 (2008) 64.
42. S. Roy, R. Banerjee, and M. Sarkar, *J. Inorg. Biochem.*, 100 (2006) 1320.
43. F. Wang, Y.X. Xu, J. Zhao, Sh.Sh. Hu, *Bioelectrochemistry* 70 (2007) 356
44. S. Niu, M. Wu, S. Bi, and S. Zhang, *Bioelectrochemistry*, 73 (2008) 64.
45. K. Maruyama, Y. Mishima, K. Minagawa, J. Motonaka, *Anal. Chem.*, 74 (2002) 3698.
46. S. Kashanian, M.M. Khodaei and P. Pakravan, *DNA Cell. Biol.*, 29 (2010) 639.
47. A.J. Bard, L.R. Faulkner, *Electrochemical Methods: Fundamentals and Applications*, Second Edition, John Wiley and Sons Publishers 2001.
48. S. Liu, M. Cao, S. Don, *Bioelectrochemistry* 74 (2008) 164.
49. R.F. Pasternack, E.J.Gibbs, J.J.Villafranca, *Biochemistry*, 22 (1983) 2406.
50. K.E. Erkkila, D.T. Odom, J. K. Barton, *Chem. Rev.*, 99 (1999) 2777.
51. C.V. Kumar, J.K. Barton, N.J. Turro, *J. Am. Chem.Soc.*, 107 (1985) 5518.
52. B.H.M. Hussein, A H. A.zab, W. Fathalla, , S. A.M.Ali, , *J. Luminesc.*, 134 (2013) 441.